J Neurophysiol 100: 2254–2264, 2008.
First published July 30, 2008; doi:10.1152/jn.90437.2008.

Persistent Sodium Current Contributes to Induced Voltage Oscillations in Locomotor-Related Hb9 Interneurons in the Mouse Spinal Cord

Lea Ziskind-Conhaim, Linying Wu, and Eric P. Wiesner
Department of Physiology and Center for Neuroscience, School of Medicine and Public Health, University of Wisconsin, Madison, Wisconsin

Submitted 4 April 2008; accepted in final form 25 July 2008

Ziskind-Conhaim L, Wu L, Wiesner EP. Persistent sodium current contributes to induced voltage oscillations in locomotor-related Hb9 interneurons in the mouse spinal cord. *J Neurophysiol* 100: 2254–2264, 2008. First published July 30, 2008; doi:10.1152/jn.90437.2008. Neurochemically induced membrane voltage oscillations and firing episodes in spinal excitatory interneurons expressing the HB9 protein (Hb9 INs) are synchronous with locomotor-like rhythmic motor outputs, suggesting that they contribute to the excitatory drive of motoneurons during locomotion. Similar to central pattern generator neurons in other systems, Hb9 INs are interconnected via electrical coupling, and their rhythmic activity does not depend on fast glutamatergic synaptic transmission. The primary objective of this study was to determine the contribution of fast excitatory and inhibitory synaptic transmission and subthreshold voltage-dependent currents to the induced membrane oscillations in Hb9 INs in the postnatal mouse spinal cord. The non-*N*-methyl-D-aspartate receptor antagonist 6-cyano-7-nitroquinoxaline-2,3-dione (CNQX) reduced the amplitude of voltage oscillations but did not alter their frequency. CNQX suppressed rhythmic motor activity. Blocking glycine and $GABA_A$ receptor-mediated inhibitory synapses as well as cholinergic transmission did not change the properties of CNQX-resistant membrane oscillations. However, disinhibition triggered new episodes of slow motor bursting that were not correlated with induced locomotor-like rhythms in Hb9 INs. Our observations indicated that fast excitatory and inhibitory synaptic inputs did not control the frequency of induced rhythmic activity in Hb9 INs. We next examined the contribution of persistent sodium current (I_{NaP}) to subthreshold membrane oscillations in the absence of primary glutamatergic, GABAergic and glycinergic synaptic drive to Hb9 INs. Low concentrations of riluzole that blocked the slow-inactivating component of sodium current gradually suppressed the amplitude and reduced the frequency of voltage oscillations. Our finding that I_{NaP} regulates locomotor-related rhythmic activity in Hb9 INs independently of primary synaptic transmission supports the concept that these neurons constitute an integral component of the rhythmogenic locomotor network in the mouse spinal cord.

INTRODUCTION

Rhythmic motor activity is generated by a specific neural circuitry in the spinal cord referred to as the locomotor central pattern generator (CPG). The autonomous CPG that is capable of producing locomotor-like rhythms independently of descending and peripheral synaptic inputs is thought to consist of ipsilateral rhythmogenic interneurons (the generators) and commissural inhibitory interneurons that coordinate the alternating rhythms between the two sides of the spinal cord. Despite the challenges in identifying interneuronal populations in the isolated mammalian spinal cord, electrophysiological and morphological studies have characterized several groups of inhibitory interneurons that are part of the rhythm-coordinating networks (e.g., Butt and Kiehn 2003; Lanuza et al. 2004; Zhong et al. 2006; reviewed by Butt et al. 2002). Considerably less is known about excitatory interneurons that might be involved in generating rhythmic excitatory drive to ipsilateral motoneurons (reviewed by Goulding and Pfaff 2005; Kiehn 2006). Two neuronal populations have been identified so far as putative CPG interneurons in genetically modified mice. Neurotransmitter agonists trigger locomotor-like rhythms in EphA4-positive neurons that are in phase with bursts of motor activity (Butt et al. 2005). Moreover, subgroups of these neurons provide mono- or polysynaptic excitatory inputs to ipsilateral motoneurons. The second group of excitatory interneurons consists of medial lamina VIII interneurons that express the homeodomain transcription factor Hb9 (Hb9 INs) (Hinckley et al. 2005a; Wilson et al. 2005). In the transgenic mouse used in these studies, the HB9 promoter controls the expression of the reporter gene green florescent protein (GFP), giving rise to GFP-expressing (GFP+) motoneurons and glutamatergic ventral interneurons. We have demonstrated that in longitudinally hemisected spinal cords with segmental ventral roots attached, neurochemically induced membrane voltage oscillations in Hb9 INs are in phase with ipsilateral rhythmic motor outputs (Hinckley et al. 2005a). Moreover, electrical coupling between clustered Hb9 INs (Hinckley and Ziskind-Conhaim 2006) and possibly other GFP+ interneurons (Wilson et al. 2007) synchronizes their rhythmic activity independently of primary fast glutamatergic transmission. Induced membrane oscillations are not confined to Hb9 INs and can be elicited in adjacent GFP+ type II interneurons that do not express the HB9 protein (Han et al. 2007).

The ability of neurons to generate subthreshold membrane oscillations derives from dynamic interactions between voltage-dependent inward and outward ionic currents and signal transduction pathways, which in turn are regulated by fast and slow synaptic mechanisms (Ramirez et al. 2004). Excitatory and inhibitory synaptic inputs play a fundamental role in controlling the onset of rhythmic firing and its termination in unidentified interneurons in the isolated rat spinal cord (Raastad et al. 1997). Similarly, excitatory synapses trigger rhythmic activity in descending commissural interneurons (Butt et al. 2002). We have shown that neurochemically induced locomo-

Address for reprint requests and other correspondence: L. Ziskind-Conhaim, Dept. of Physiology, School of Medicine and Public Health, 129 SMI, 1300 University Ave., University of Wisconsin, Madison, WI 53706 (E-mail: lconhaim@physiology.wisc.edu).

The costs of publication of this article were defrayed in part by the payment of page charges. The article must therefore be hereby marked "*advertisement*" in accordance with 18 U.S.C. Section 1734 solely to indicate this fact.

tor-like voltage oscillations and rhythmic firing are correlated with episodes of increased frequency of excitatory postsynaptic potentials (EPSCs) in both Hb9 INs and GAD67/GFP-expressing commissural interneurons (Hinckley et al. 2005a; Wu and Ziskind-Conhaim 2006). Blocking fast non-NMDAR-mediated synaptic transmission suppresses rhythmic activity in GAD67/GFP-expressing inhibitory interneurons but not in Hb9 INs. Activation of voltage-dependent inward currents or termination of outward currents can trigger rhythmic membrane depolarizations but to date little is known about the identity of the ionic currents that underlie rhythmic activity in Hb9 INs. One report has proposed that low-voltage-activated (LVA) calcium current contributes to neurochemically induced large voltage oscillations in a fraction of Hb9 INs in spinal cord slices of juvenile mice (Wilson et al. 2005).

The primary objectives of our study were to distinguish between synaptic and cellular mechanisms responsible for neurochemically induced locomotor-like rhythms in Hb9 INs in hemisected spinal cords of postnatal mice. Our observations demonstrated that in the absence of primary excitatory and inhibitory synaptic transmission, persistent sodium current (I_{NaP}) played an important role in controlling the pattern of locomotor-like voltage oscillations in this distinct population of excitatory interneurons.

METHODS

Spinal cord preparation

Experiments were performed using the HB9/eGFP transgenic mouse line (Wichterle et al. 2002). Newborn mice (P1–P4) were anesthetized by hypothermia, and after decapitation, the spinal cord was extracted in ice-cold oxygenated dissection solution as described previously (Hinckley et al. 2005b). The cord with ventral roots T_{12}–S_2 attached was equilibrated in extracellular solution at room temperature for 30 min. The spinal cord was then transferred to a silicone-elastomer (Sylgard)-coated recording chamber, where it was continuously superfused with oxygenated extracellular solution at a rate of 2–5 ml/min at room temperature.

Simultaneous ventral root and whole cell recordings

The procedures for simultaneous ventral root and whole cell recordings were identical to those described recently (Hinckley et al. 2005a). Locomotor-like rhythms were produced by a mixture of 5-HT, *N*-methyl-DL-aspartate (NMA), and dopamine (the "rhythmogenic cocktail"). Variable agonist concentrations were required to initiate locomotor-like rhythms, but unless stated differently, stable alternating rhythms were triggered with 5 μM NMA, 10 μM 5-HT, and 50 μM dopamine. To monitor motor activity, ventral roots were drawn into bipolar, tight-fitting suction pipettes. Ventral root recordings were band-pass filtered between 300 Hz and 1 kHz, and the output from the AC amplifier (M50, World Precision Instruments) was acquired at a sampling rate of 2–3 kHz. The sampling rate was 10 kHz when ventral root and Hb9 IN potentials were recorded simultaneously. When quasi-DC recording were performed, the cutoff of the high-pass filter was reduced to 0.1 Hz. Electroneurograms of rhythmic motor activity alternating between left-right L_2 ventral roots (flexor-related) and ipsilateral L_5 ventral roots (extensor-related) (Kiehn and Kjaerulff 1996) confirmed that the induced rhythms were related to locomotor activity.

The spinal cord was then transected longitudinally and was placed in a glass-covered recording chamber with the medial side up so that GFP+ Hb9 INs could be visually identified for whole cell patch-clamp recordings. We used a fluorescence microscope (Olympus, BX50WI) equipped with a 475-nm excitation filter, a 505-nm dichoric mirror, and a 535-nm emission filter (Omega Optics) to place the patch pipettes (tip resistances of 5–7 MΩ, P-97 multi-stage puller, Sutter Instrument) above the cell body of Hb9 INs. The distinct shape of the small Hb9 INs, their clustering in medial lamina VIII and their visible primary ventral and dorsal dendrites facilitated their morphological identification (Hinckley et al. 2005a). Electrophysiological criteria were used to confirm their identity (see RESULTS). To obtain whole cell recording using videomicroscopy, the fluorescence was switched to infrared-differential interference contrast optics (Ziskind-Conhaim et al. 2003). Intracellular potentials/currents were filtered at 3 kHz, sampled at 10–20 kHz (Multiclamp 700B amplifier, Molecular Devices) and recorded on a PC with Clampex software (v9.2). Interneurons were included in the study only if their resting membrane potential was more negative than −50 mV and action potential peak amplitude overshot zero. For voltage-clamp recordings, whole cell capacitance transients were canceled on-line and monitored throughout the experiment. Series resistance was compensated to 60–80%. All recordings were corrected off-line for a liquid junction potential of 10 mV (Gao et al. 2001).

Data analysis

The cycle period of membrane oscillation was defined as the time between the onset of two consecutive subthreshold membrane depolarizations. Averages of amplitude and cycle period were calculated based on 10–20 successive membrane oscillations. Data are presented as averages ± standard errors (SE). Paired *t*-test were used to determine the statistical significance ($P < 0.05$). Statistics of circular distribution was used to correlate the phase relations between whole cell subthreshold rhythms and ventral root recordings. To obtain the phase, the onset of membrane depolarization was subtracted from the onset of ventral root burst and divided by the cycle period of the root discharge. Twenty successive cycles were analyzed yielding values from zero to one. Individual values were plotted on a circle, and the mean phase was represented with a vector. For values from 0 to 1, 0 indicated in phase correlation while 0.5 marked an out-of-phase correlation. The length of the vector is inversely proportional to the distribution of individual phase values around the mean. The significance of the mean was calculated from the length of the vector (*r*) using Rayleighs test (Zar 1974).

Solutions and chemicals

Extracellular solution contained (in mM) 128 NaCl, 4 KCl, 1.5 $CaCl_2$, 1 $MgSO_4$, 0.5 NaH_2PO_4, 21 $NaHCO_3$, and 30 glucose. The solution was adjusted to pH 7.3 using NaOH, and the osmolarity was 315–325 mosM. Dissection solution had similar composition, but $CaCl_2$ concentration was lower (0.5 mM), and $MgSO_4$ concentration was higher (6 mM). The whole cell pipette solution contained (in mM) 140 K gluconate, 9 KCl, 10 *N*-(2-hydeoxyethyl)piperazine-*N*′-(2-ethanesulfonic acid) (HEPES), 0.2 ethylene glycol-bis(2-aminoethylether)-*N,N,N′,N′*-tetraacetic acid (EGTA), 1 Mg-ATP, and 0.1 GTP. The solution was adjusted to pH 7.2 using KOH, and the osmolarity was 290–305 mosM. All chemicals were obtained from Sigma.

RESULTS

Experiments were performed in the longitudinally hemisected spinal cord in which visually identified Hb9 INs were targeted for whole cell recordings, and their activity was correlated with electroneurograms of segmental ventral roots. In this study, GFP+ neurons were identified as Hb9 INs based on the following criteria: *1*) small-diameter neurons clustered in medial lamina VIII, *2*) high-input resistance, ranging from 800 to 1,300 MΩ, *3*) linear *I-V* relation without hyperpolarization-dependent depolarization sag, *4*) small rheobase: 5–15 pA,

and *5*) spike frequency adaptation during repetitive firing in response to a prolonged depolarizing voltage step. Recordings were discontinued from neurons with different electrophysiological properties. Low-frequency spontaneous excitatory and inhibitory postsynaptic potentials (0.1–2.0 Hz) and infrequent firing characterize Hb9 INs. This is in sharp contrast to tonic firing in other GFP+ and GFP− interneurons in medial lamina VIII. We could not use tonic firing as a criterion to distinguish between Hb9 INs and other neurons in the area because most recordings were carried out after neurochemically induced subthreshold oscillations and rhythmic firing were established. Hb9 INs are not intrinsically rhythmic under control conditions, but two to three cycles of membrane voltage oscillations (cycle period: 5–8 s) and rhythmic firing can be recorded periodically (e.g., Fig. 6 in Hinckley and Ziskind-Conhaim 2006). Some or all of these criteria have been used in previous studies to distinguish between type I (Hb9) and type II interneurons (Han et al. 2007; Hinckley and Ziskind-Conhaim 2006; Hinckley et al. 2005a; Wilson et al. 2005, 2007). Approximately half the Hb9 INs (n = 19/47) were labeled with neurobiotin to confirm their morphological properties (Hinckley et al. 2005a). Expression of the HB9 protein is the best criterion that classifies a neuron as Hb9 IN and distinguishes it from neighboring GFP+ interneurons. However, as we reported previously, staining with the HB9 antibody gradually weakens during prolonged whole cell recordings, and it cannot be detected in experiments that last >30 min (Hinckley et al. 2005a).

The mixture of NMA, 5-HT, and dopamine, the rhythmogenic cocktail, triggered rhythmic motor activity in ~80% of the spinal cords. Electroneurograms of motor outputs alternating between left-right L_2 or L_3 ventral roots or between ipsilateral L_2 and L_5 ventral roots (Hinckley et al. 2005a) confirmed that those were locomotor-like rhythms. When rhythmic activity was established in the intact spinal cord, the cord was sectioned longitudinally along the midline. Rhythmic motor activity persisted in only ~50% of the cords following the longitudinal section. Membrane voltage oscillations in phase with rhythmic motor activity were recorded in 83% of Hb9 INs (n = 15/18). Therefore neurochemically induced locomotor-like rhythms were recorded in approximately one Hb9 IN of every three spinal cords.

Blocking fast excitatory and inhibitory synaptic transmission did not alter the frequency of locomotor-like voltage oscillations in Hb9 INs

Under control conditions and during induced rhythmic activity, primarily fast-rising, fast-decaying EPSCs were recorded at various holding potentials (ranging from −40 to −60 mV), and these were blocked by 6-cyano-7-nitroquinoxalene-2,3-dione (CNQX, 10 μM), a non-NMDA receptor (non-NMDAR) antagonist (Fig. 1*A*, n = 5). We used the term fast glutamatergic transmission when referring to non-NMDAR-mediated EPSCs because of their significantly faster kinetics than those of NMDAR-mediated EPSCs (Ziskind-Conhaim et al. 2003). Slow-rising, slow-decaying EPSCs that are indicative of NMDAR-mediated synaptic currents were not evident at holding potentials more negative than −40 mV. We have recently reported that CNQX does not block neurochemically induced membrane voltage oscillations in Hb9 INs, but it suppresses rhythmic firing in motoneurons (Hinckley and Ziskind-Conhaim 2006). To examine whether CNQX blocked voltage oscillations in motoneurons, quasi-DC recordings were performed to monitor ventral root potentials. Our observation that the antagonist blocked motoneuron oscillatory activity (Fig. 1*B*) indicated that rhythmic activity in motoneurons was dependent on non-NMDAR-mediated synaptic transmission.

To determine the role of excitatory postsynaptic potentials (EPSPs) in rhythm initiation, we examined the effect of CNQX on the amplitude neurochemically induced membrane voltage oscillations. Exposure to CNQX reduced the amplitude from 11.7 ± 0.8 mV (n = 8) to 7.7 ± 1.1 mV, but there was no change in the oscillation frequency (Fig. 2, *A* and *C*). The smaller CNQX-resistant oscillations were associated with lower firing rates. NMDA receptors were not blocked because NMA was one of the agonists used to trigger rhythmic activity in the hemicord preparation. In the presence of CNQX, rhythmic motoneuron activity was converted to tonic firing.

To examine whether voltage oscillations could be generated if fast synaptic transmission was blocked before adding the

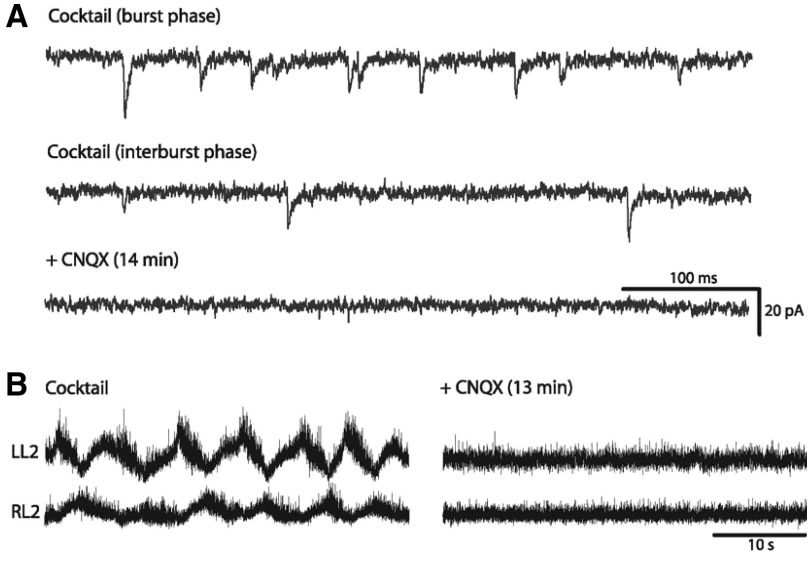

FIG. 1. Blocking non-*N*-methyl-D-aspartate receptor (non-NMDAR)-mediated synaptic transmission suppressed both excitatory synaptic currents in Hb9 interneurons (Hb9 INs) and voltage oscillations in motoneurons. *A*: primarily fast-rising, fast-decaying excitatory postsynaptic currents (EPSCs) were recorded during the burst and interburst phases of membrane oscillations. The EPSCs were blocked after a 14-min exposure to 6-cyano-7-nitroquinoxalene-2,3-dione (CNQX) (10 μM). *B*: the rhythmogenic cocktail triggered voltage oscillations in L2 motoneurons that alternated between the left-right sides of the intact spinal cord (quasi-DC ventral root recordings). The oscillatory motor output was blocked within 13 min of CNQX application.

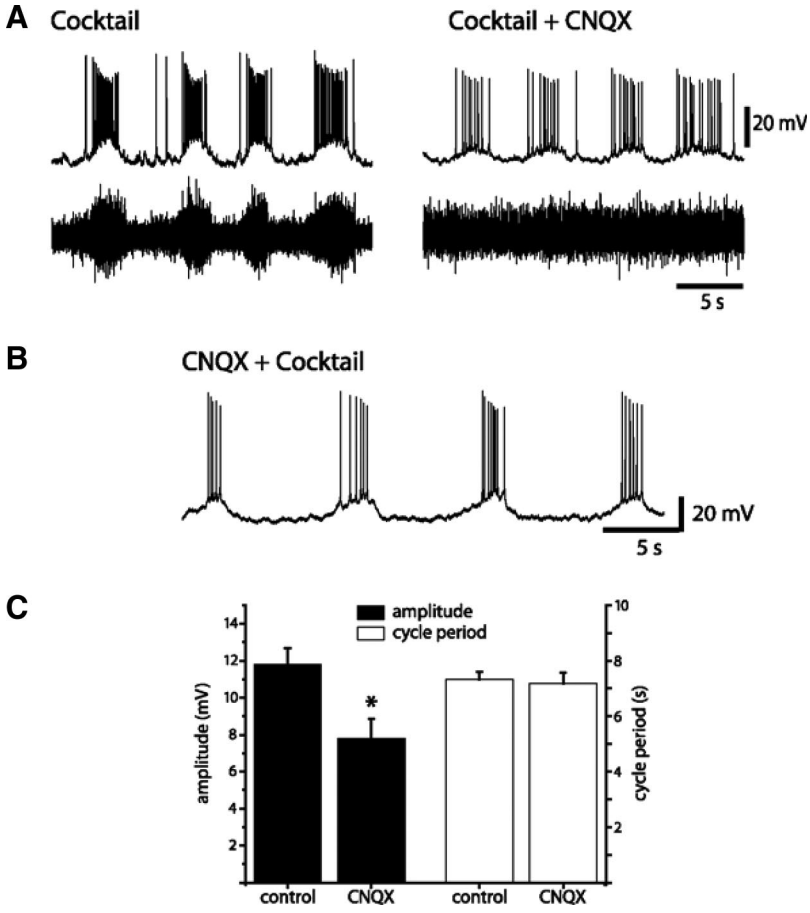

FIG. 2. Suppressing non-NMDAR-mediated synaptic inputs reduced the amplitude of locomotor-like oscillations in Hb9 INs but did not alter their frequency. *A*: simultaneous recording of cocktail-induced locomotor-like rhythms in Hb9 IN (*top trace*) and electroneurograms of L2 ventral root (*bottom trace*). Membrane voltage oscillations and firing in Hb9 IN were in phase with ventral root bursts. Membrane potential: −52 mV. Same frequency oscillations persisted in Hb9 IN after adding CNQX (10 μM, cocktail+CNQX), but blocking non-NMDAR-mediated synaptic transmission converted ventral root bursts to tonic activity. CNQX did not block the small, irregular fluctuations in membrane potential that were apparent in the presence of the rhythmogenic agonists. In the example shown, the noise level of ventral root recording increased after adding CNQX, which might reflect a slight shift in the root position in the suction electrode. *B*: similar membrane oscillations were apparent in a different Hb9 IN in which non-NMDAR-mediated transmission was blocked *before* adding the cocktail (CNQX+cocktail). Membrane potential: −55 mV. *C*: histogram of the mean amplitude and cycle period of voltage oscillations (mean ± SE) in control and CNQX-containing solutions showed that the average amplitude significantly decreased from 11.7 ± 0.8 mV ($n = 8$) to 7.7 ± 1.1 mV. The reduced amplitude was associated with lower firing rate that decreased from an average of 8.2 Hz (control) to 3.3 Hz (CNQX). CNQX did not alter the cycle period. *Significantly smaller than control $P > 0.04$.

rhythmogenic cocktail, the intact spinal cord was exposed to CNQX for 15 min *before* applying the cocktail of neurotransmitter agonists. Recordings from Hb9 INs were performed following a 40-min exposure to both CNXQ and the cocktail. The effectiveness of the agonists in triggering rhythmic motor outputs could not be evaluated in the presence of CNQX (Fig. 1*B*). When non-NMDARs were blocked before applying the mixture of neurotransmitter agonists, rhythmic activity was expected in about one Hb9 IN of every three spinal cords tested (see preceding text). Under these conditions, neurochemically induced CNQX-resistant membrane oscillations were recorded in 2/7 Hb9 INs (Fig. 2*B*, $n = 3$ spinal cords), suggesting that fast glutamatergic transmission was not required to trigger rhythmic activity in these interneurons.

The frequency of inhibitory postsynaptic currents (IPSCs) is low in Hb9 INs in the hemisected spinal cord, and it does not change during the cycle period (Hinckley et al. 2005a). The assumption that inhibitory synaptic transmission did not influence burst and interburst durations was tested by investigating the effect of disinhibition on CNQX-resistant rhythmic activity. IPSCs were suppressed by adding picrotoxin (Picro, 10 μM, $n = 5$) or bicuculline (5 μM, $n = 1$), $GABA_A$ receptor ($GABA_AR$) antagonists, and strychnine (Str, 0.5 μM, $n = 6$), a glycine receptor (GlyR) antagonist. Disinhibition did not significantly alter the amplitude or cycle period of neurochemically induced CNQX-resistant membrane oscillations in Hb9 INs (Fig. 3, *A* and *B*). However, suppressing inhibitory transmission triggered new episodes of motor bursting that were not correlated with the faster voltage oscillations in Hb9 INs (Fig. 3*B,* circular phase diagram). These motor rhythms were different from the *spontaneous, irregular* long- and short-duration bursts of motor activity that was produced by blocking fast inhibitory transmission in the absence of rhythmogenic agonists (see Fig. 2 in Hinckley et al. 2005b). The average cycle period of neurochemically induced motoneuron rhythms was 20.3 ± 2.9 s ($n = 6$), approximately threefold longer than episodes of motor bursts generated before blocking non-NMDARs (Fig. 2*A,* cocktail). The average cycle period of CNQX-resistant, disinhibition-induced motor bursts in the hemicord (Fig. 3) was similar to that of rhythmic motor outputs in the intact spinal cord in which glycinergic and GABAergic transmission but not non-NMDAR-mediated synapses were blocked (26.9 ± 4.9 s) (Hinckley et al. 2005b). Therefore it is reasonable to propose that in the absence of fast glutamatergic and inhibitory inputs, different synaptic and/or cellular mechanisms were responsible for the induced rhythmic activities in Hb9 INs and motoneurons.

Cholinergic transmission modulates the activity of locomotor networks in vertebrates (e.g., Cowley and Schmidt 1994; Quinlan et al. 2004), and it increases the firing rate of ascending commissural interneurons in the neonatal mouse spinal cord (Carlin et al. 2006). Therefore it was important to investigate whether cholinergic inputs could influence neurochemically induced voltage oscillations that persisted in the presence of CNQX, Str, and Picro. In this and all other experiments described in the following text, CNQX was bath-applied first (Figs. 2*A* and 3*A*), and only after it blocked rhythmic motor activity were Picro and Str added to the extracellular solution.

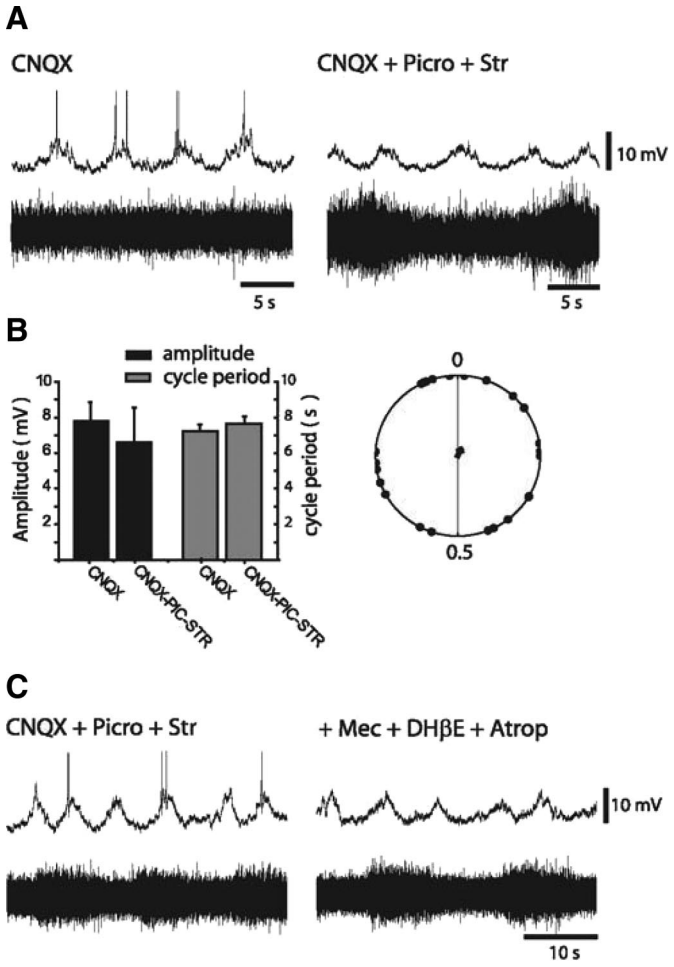

FIG. 3. *A*: blocking fast inhibitory and cholinergic transmission did not alter the properties of induced membrane oscillations in Hb9 INs. *A*: the amplitude and frequency of induced CNQX-resistant voltage oscillations did not change after blocking glycinergic and GABAergic transmission [CNQX + picrotoxin (Picro) + strychnine (Str)], but disinhibition converted tonic motoneuron firing into new episodes of slow bursting. In this and all other figures, CNQX was applied 1st and the mixture of Picro and Str was added only after CNQX suppressed motor activity (~15 min). Membrane potential: −56 mV. Action potentials are truncated. *B*: histogram of the amplitude and cycle period (mean ± SE, $n = 6$) as a function of blocking non-NMDARs (CNQX) or suppressing both fast excitatory and inhibitory transmission (CNQX+Picro+Str). Disinhibition did not significantly change the amplitude CNQX-resistant membrane oscillations. Cycle periods of 7.3 s (CNQX) and 7.6 s (CNQX+Picro+Str) in Hb9 INs were significantly faster than bursts of motor outputs (cycle period, 20.3 s). Circular phase analysis was performed to evaluate the correlation between membrane oscillations and ventral root bursts. The diagram demonstrated broadly distributed phase values, reflecting the lack of correlation between rhythmic activities in Hb9 INs and motoneurons. The small arrow described the insignificant concentration of the phase value around the mean ($r = 0.12$). *C*: blocking nicotinic and muscarinic receptors did not significantly alter the properties of membrane oscillations in Hb9 INs, but it increased the cycle period of motor rhythms from 14 to 20 s. The increase was attributed to longer interburst duration. Membrane potential: −50 mV. Action potentials are truncated.

Nicotinic and muscarinic receptor antagonists were applied after neuronal disinhibition triggered slow motor output bursts. Cholinergic transmission was suppressed by mecamylamine (Mec, 10 μM), dihydro-beta-erythroidine (DHβE, 50 μM), d-tubocurarine (10 μM, $n = 2/4$ experiments), and atropine (Atrop, 10 μM), blockers of nicotinic and muscarinic receptors. Suppressing cholinergic transmission did not alter the pattern of induced rhythmic activity in Hb9 INs (Fig. 3*C*, $n = 4$), but it increased the interepisode intervals of motor bursts by 2–5 s, thus slowing the rhythms. Our finding that the frequency of locomotor-like rhythms in Hb9 INs was not altered after blocking primary excitatory and inhibitory synaptic inputs implied that fast synaptic transmission did not play an important role in eliciting rhythmic activity in this population of locomotor-related interneurons.

In the series of experiments described in the following text, we used the term "synaptically isolated Hb9 INs" to describe rhythmic activity during the blockade of EPSCs with CNQX and IPSCs with strychnine and picrotoxin.

Persistent sodium current contributed to membrane oscillations in Hb9 INs

The ability of a neuronal population to generate rhythmic membrane depolarizations depends on voltage-gated ionic currents and/or slow synaptic transmission. One of the candidates for generating membrane voltage oscillations is I_{NaP}, a subthreshold, slow-inactivating current that has been shown to participate in rhythmic activity in other networks. For example, in neurons in the respiratory pre-Bötzinger complex, the ratio between persistent sodium and potassium-dominant leak conductances is significantly higher in intrinsically bursting than in nonbursting neurons (Koizumi and Smith 2008). I_{NaP} contributes to spike initiation produced by slow inputs in ventral neurons in the mammalian spinal cord (Theiss et al. 2007), and blocking it suppresses rhythmic firing in locomotor-related commissural interneurons in the neonatal mouse spinal cord (Zhong et al. 2007). To assess the contribution of I_{NaP} to induced voltage oscillations in Hb9 INs, rhythmic activity was examined in the presence of riluzole (Ril), a blocker of the persistent component of the sodium current (Urbani and Belluzzi 2000). In the first set of experiments, we studied the effect of Ril on tonic firing evoked by a prolonged depolarizing voltage step. At low concentrations (5–10 μM) that effectively blocked I_{NaP} (Kuo et al. 2006), Ril converted repetitive firing to a single action potential (Fig. 4*A*, $n = 6$). As reported previously (e.g., Zhong et al. 2007), tonic firing was suppressed gradually and became apparent only after a 30- to 40-min exposure to the blocker, probably because Ril is lipophilic in nature and diffuses slowly into the tissue.

We next investigated the basic properties of I_{NaP}. The current was generated by a slowly rising voltage command that was applied at a rate adjusted to avoid action potential generation (Fig. 4*B*). Sodium current was isolated by blocking the majority of potassium and calcium currents with tetraethylammonium (TEA, 10 mM), 4-aminopyridine (4-AP, 4 mM) and $CdCl_2$ (300 μM) in the extracellular solution, and Cs-gluconate replaced K-gluconate in the pipette solution. Under these conditions, the currents generated in Hb9 INs revealed a region of negative slope in the *I-V* function that was blocked by Ril (Fig. 4*B*). The current was activated at −55.2 ± 1.4 mV (SE, $n = 6$) and peaked at −42.6 ± 2.2 mV. To estimate the peak amplitude of the inward current, measurements were carried out after filtering (200 Hz), the recorded traces to reduce the high-frequency noise without distorting the current waveform. The average amplitude of I_{NaP} estimated in this manner was −15.4 ± 1.5 pA, ranging from 10 to 19 pA. This is a small current, but theoretically it can produce membrane depolariza-

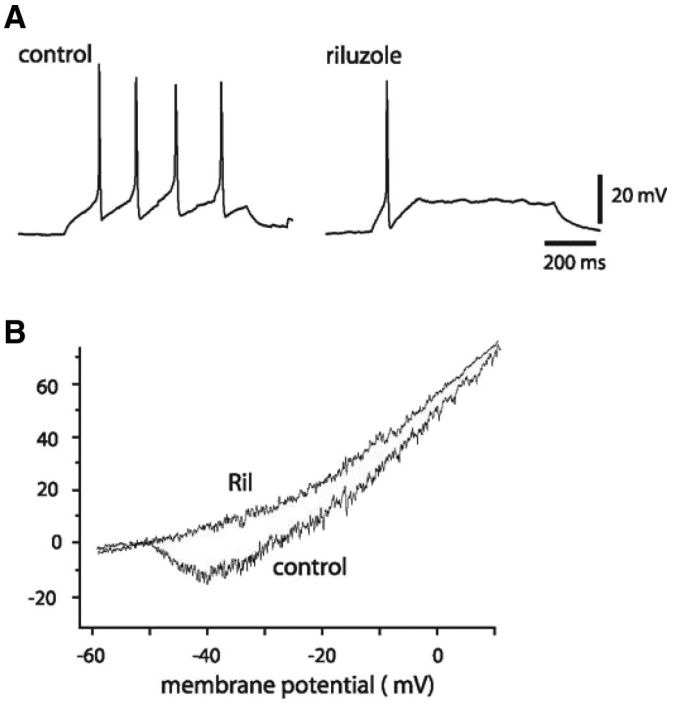

FIG. 4. I_{NaP} contributed to repetitive firing in Hb9 INs. *A*: repetitive firing generated by a prolonged depolarizing current step (7 pA/800 ms) was converted to a single action potential after 32-min exposure to riluzole (Ril, 5 μM). Membrane potential: −60 mV. *B*: in a different Hb9 IN, cadmium-resistant inward current that was generated in response to a slow depolarization ramp from −70 to +10 mV at a rate 80 mV/3 s. The current was blocked by Ril (10 μM). I_{NaP} was activated at −51 mV, and the peak amplitude was −17.2 pA at membrane potential of −42 mV.

tions of ~15 mV in Hb9 INs with typical input resistance of ~1 GΩ.

To determine the role of I_{NaP} in generating locomotor-like voltage oscillations in synaptically isolated Hb9 INs, we studied the Ril effect on neurochemically induced rhythmic activity. After a long exposure, the I_{NaP} blocker suppressed membrane voltage oscillations in Hb9 INs (Fig. 5*A*). Within ~30–35 min of Ril application, their amplitude decreased from 5.9 ± 0.6 mV (n = 3) to 3.5 ± 1.2 mV, and the frequency was reduced from 0.13 ± 0.01 to 0.07 ± 0.01 Hz. Oscillations were typically blocked within 35–40 min. Qualitative observations revealed that the amplitude of rhythmic motor activity was also gradually suppressed by Ril (Fig. 5*A*), but unlike the oscillations in Hb9 INs, the frequency of ventral root bursts remained relatively unchanged until the bursts were no longer detectable. These findings suggested that I_{NaP} played a different role in mediating induced rhythmic activity in synaptically isolated Hb9 INs and motoneurons.

To investigate whether the rhythmogenic cocktail altered the threshold and/or amplitude of I_{NaP}, we examined its effect on I_{NaP} in synaptically isolated Hb9 INs (Fig. 5*C,* control). The blockers of fast excitatory and inhibitory synaptic transmission (CNQX, Picro, and Str) did not significantly change the threshold and amplitude of I_{NaP} (not shown, n = 5). At concentrations that characteristically induced locomotor-like rhythms, the mixture of neurotransmitter agonists significantly increased the amplitude of the inward current from an average of 12.5 ± 1.7 pA (SE, n = 4) to 17.0 ± 2.2 pA. Therefore it is conceivable that the agonists facilitated the onset of voltage oscillations by increasing the amplitude of $I_{NaP.}$ However, we cannot rule out the possibility that the increase in inward current was attributable to somatic NMDA receptors that could be partially activated at comparable membrane potentials.

Previous reports have demonstrated that TTX, which effectively blocks the persistent component of the sodium current (e.g., Koizumi and Smith 2008), does not suppress neurochemically induced rhythmic membrane depolarizations in Hb9 INs in spinal cord slices of P1–P7 and juvenile mice (Han et al. 2007; Wilson et al. 2005). Therefore, it was important that we examine its action on induced locomotor-like rhythms in Hb9 INs in the hemisected spinal cord. In contrast to the reported TTX-resistant rhythmic depolarizations, in our experiments, TTX blocked membrane oscillations in synaptically isolated Hb9 INs (Fig. 5*B, n* = 2). TTX inhibitory action was significantly faster than that of Ril, but similar to Ril, the gradual decrease in amplitude was in concert with slower frequencies. Although these observations support our conclusion that the slow component of the sodium current participates in subthreshold membrane oscillations, we cannot rule out the possibility that TTX blocked slow synaptic transmission and suppressed the release of neuromodulators that might play a role in regulating rhythmic activity.

One of the main differences between our experimental procedures and the protocols used to trigger TTX-resistant membrane oscillations is the significantly higher concentration of NMDA in the cocktail that triggered oscillations in the latter studies. Therefore we repeated some of the experiments using rhythmogenic cocktail that contained 20 μM NMDA, 20 μM 5-HT, and 50 μM dopamine (Han et al. 2007; Wilson et al. 2005) instead of 5 μM NMA, 10 μM 5-HT, and 50 μM dopamine. The protocol for inducing rhythms in synaptically isolated hemicord was identical to that used with low concentration of NMA, but motor activity was not monitored. Similar to the reports cited in the preceding text, exposure to high concentrations of NMDA triggered large membrane oscillations (>20 mV) at frequencies that varied from 0.2 to 0.4 Hz (Fig. 6*A, n* = 5). In the presence of TTX (1 μM, 5 min), their amplitude was significantly reduced from 29.7 ± 0.9 mV (n = 3) to 14.6 ± 1.2 mV (Fig. 6, *C* and *D*), but their frequency did not decrease, remaining at an average of 0.3 ± 0.06 Hz. In the presence of high NMDA, TTX did not block voltage oscillations in synaptically isolated Hb9 INs. Our data implied that voltage oscillations induced by low concentrations of NMA are controlled by I_{NAP}, but different cellular mechanism(s) underlie rhythmic activity triggered by high concentration of NMDA.

Nickel suppressed rhythmic activity in Hb9 INs

LVA calcium current regulates burst frequency in the locomotor circuitry in the lamprey (Tegnér et al. 1997), and it has been proposed that it contributes to neurochemically induced TTX-resistant rhythmic membrane depolarizations in a fraction of Hb9 INs in spinal cord slices of juvenile mice (Wilson et al. 2005). In the latter study, only the large oscillations (>40 mV) were voltage-dependent and blocked by nickel (100 μM). Although nickel is not a specific blocker, it is more effective inhibiting LVA calcium current than N- and L-type calcium currents. To determine whether nickel had a similar effect on the smaller (<15 mV) and slower (0.1–0.2 Hz) locomotor-like

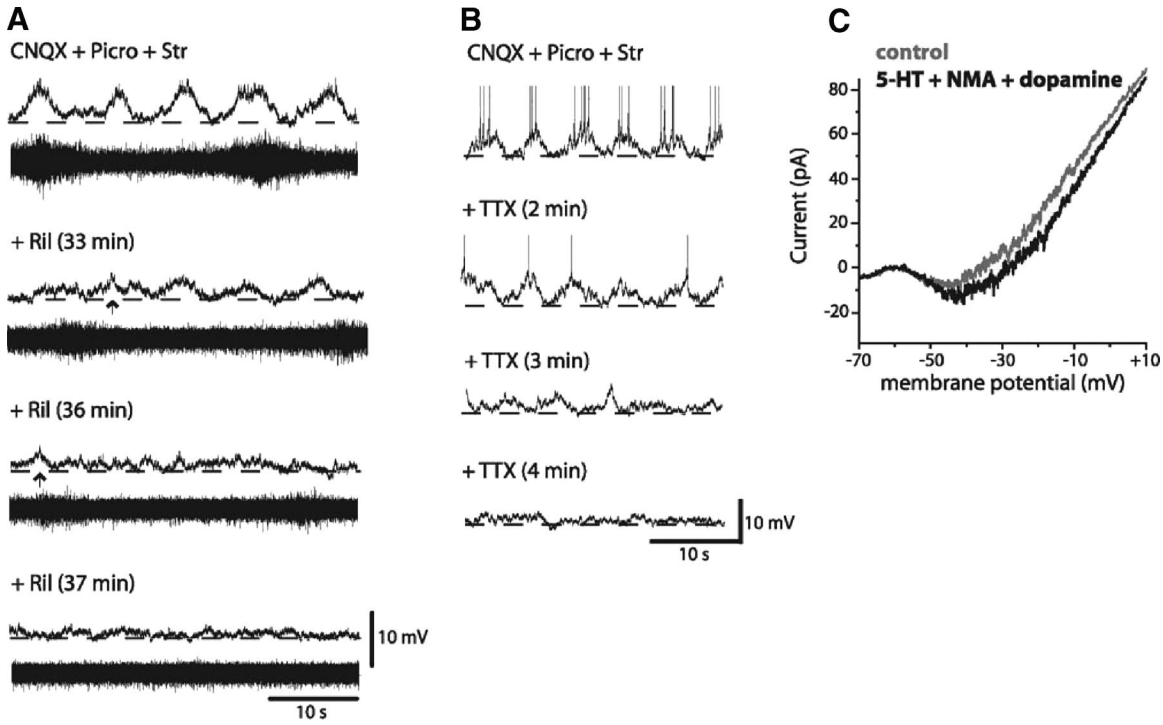

FIG. 5. Ril and TTX suppressed rhythmic activity in Hb9 INs and motoneurons. *A*: in a synaptically isolated Hb9 IN (CNQX + Picro + Str), the average amplitude of induced locomotor-like voltage oscillations was 5.2 ± 0.3 mV (SE, $n = 10$ cycles) and their frequency was 0.12 Hz. Smaller (2.8 ± 0.3 mV) and slower oscillations (0.09 Hz) were recorded after 33-min exposure to Ril (10 μM). The amplitude of voltage oscillations and their frequency gradually decreased and 36 min after Ril application the amplitude was 1.9 mV at frequency of 0.02 Hz. After 37 min, the induced oscillations were no longer detectable. Membrane potential: −50 mV. The frequency was determined during a period of 10 cycles. In this and all subsequent figures, during pharmacological manipulation that reduced the amplitude and frequency of rhythmic activity, subthreshold depolarizations were identified as membrane oscillations if their amplitude and duration were ≥33 and 75% of control values, respectively. Examples of membrane depolarizations that were included in the analysis are marked by arrows. The amplitude of the slow ventral root bursts gradually decreased but their frequency (0.04 Hz) was not altered until bursts were no longer measurable (37 min). *B*: in a different Hb9 IN, a brief exposure to TTX (1 μM, 2 min) slightly reduced the amplitude and frequency of membrane oscillations from 7.9 ± 0.8 mV (SE, $n = 10$ cycles) at 0.17 Hz to 6.5 ± 0.5 mV at 0.15 Hz. A significant decrease in amplitude (4.4 ± 1.4 mV, $n = 4$) and slower frequency (0.08 Hz) were recorded after 3-min exposure to the toxin. Voltage oscillations were suppressed within 4 min of TTX application. Membrane potential: −60 mV. Action potentials are truncated. *C*: comparison of the currents generated in response to a slow depolarization ramp (80 mV/3 s) in the presence of CNQX, Picro and Str (control) and after adding NMA (5 μM), 5-HT (10 μM), and dopamine (50 μM). In the synaptically isolated Hb9 IN, the amplitude of the inward current increased by 6 pA in the presence of the cocktail.

rhythms recorded in Hb9 INs in the hemicord, we studied its effect on induced voltage oscillations. Unlike the data presented in the study cited in the preceding text, nickel blocked the relatively small oscillations (Fig. 7*A*, $n = 5$). The gradual decrease in amplitude oscillations was associated with a parallel reduction in their frequency. Within 3- to 4-min exposure to nickel, the amplitude of voltage oscillations was significantly reduced from 5.7 ± 0.8 mV ($n = 4$) to 3.1 ± 0.5 mV, whereas the frequency was reduced from 0.13 ± 0.03 to 0.08 ± 0.01 Hz. Nickel had a similar action on rhythmic firing in motoneurons. Nickel blocked rhythmic activity in both Hb9 INs and motoneurons, suggesting that LVA calcium current participated in neurochemically induced rhythms in both neuronal populations. To test this hypothesis, we examined the voltage-dependent behavior of membrane oscillations. LVA calcium currents are partially inactivated at resting membrane potential and their amplitude should increase with membrane hyperpolarization. The results of these experiments were inconsistent in part because during induced rhythmic activity it was difficult to clamp the membrane at hyperpolarizing or depolarizing potentials for periods >40–60 s, because membrane potentials gradually drifted back toward −50 to −60 mV ($n = 4$). Frequently, after prolonged (>20 s) hyperpolarizations to potentials more negative than −80 mV, membrane potentials became unstable, resulting in abrupt depolarizations to potentials more positive than −40 mV.

We also examined the action of nickel on the large voltage oscillations triggered by high concentration of NMDA (20 μM, Fig. 7*B*). Similar to its action on the small voltage oscillations induced by low concentration of NMA (5 μM) in the rhythmogenic cocktail, nickel gradually decreased both the amplitude and frequency of the large oscillations ($n = 3$). Within 14 min of nickel application, the amplitude was reduced from 14.0 to 4.1 mV with a parallel decrease in the frequency from 0.23 to 0.13 Hz.

DISCUSSION

Locomotion is a phasic motor activity, often executed for only a few rhythmic cycles, therefore it is debatable (reviewed by Getting 1989) whether locomotor rhythms are generated by neurons with rhythmogenic properties similar to those of the intrinsic bursters in the pre-Bötzinger complex that contribute to respiratory rhythm generation (Rekling and Feldman 1998; Smith et al. 1991; Tryba et al. 2003). Hb9 INs are not intrinsically rhythmic neurons (Han et al. 2007), but infrequent spontaneous episodes of membrane voltage oscillations similar to those induced by the rhythmogenic cocktail are detected

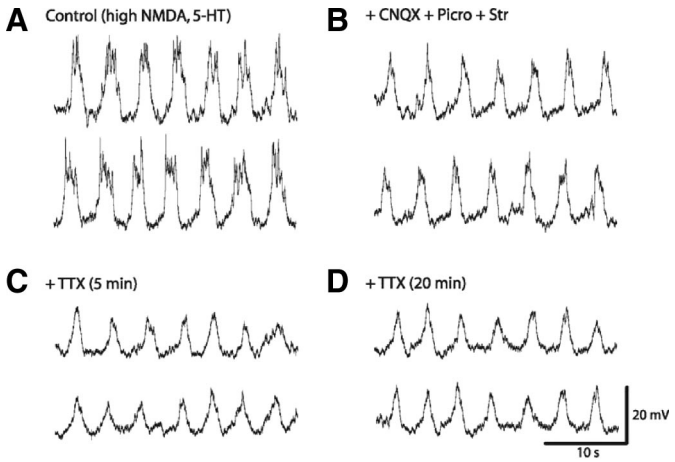

FIG. 6. TTX-resistant membrane voltage oscillations generated in a Hb9 IN by rhythmogenic cocktail containing high concentrations of NMDA and 5-HT. *A*: large membrane oscillations (31 ± 0.6 mV, SE, $n = 20$ cycles) at frequency of 0.24 Hz were triggered by 20 μM NMDA, 20 μM 5-HT, and 50 μM dopamine. *B*: after blocking fast synaptic transmission (CNQX + Picro + Str), their amplitude was significantly reduced to 23.9 ± 0.5 mV, but their frequency did not change. *C*: adding TTX (1 μM, 5 min) did not alter the frequency but further decreased the amplitude to an average of 14.6 ± 0.4 mV. *D*: the induced oscillations persisted after a long exposure to TTX (20 min) when the average amplitude was 15.2 ± 0.4 mV at a frequency of 0.24 Hz. Membrane potential: −60 to −65 mV. The *top* and *bottom traces* in *A–D* are part of continuous recordings under the different experimental conditions.

periodically (Hinckley and Ziskind-Conhaim 2006). Our findings that subthreshold persistent sodium current and possibly LVA calcium current participate in neurochemically induced locomotor-like membrane oscillations in the absence of primary excitatory and inhibitory synaptic drive, support the concept that Hb9 INs are part of the locomotor CPG (reviewed by Kiehn 2006). However, the function of this neuronal population in the rhythmogenic locomotor network is for the most part unknown.

Fast synaptic transmission does not control the frequency of locomotor-like voltage oscillations in Hb9 INs

The locomotor CPG can function in relative autonomy, but its excitation in vivo is regulated by the reticulospinal neurons in the lower brain stem (Arshavsky et al. 1984; Atsuta et al. 1990; Noga et al. 1991) and peripheral inputs (Burke et al. 2001; reviewed by Hultborn et al. 1998; McCrea 2001). The autonomous locomotor CPG is capable of generating rhythmic motor outputs independently of descending and peripheral inputs, making the isolated spinal cord a valuable preparation for studying the functions of locomotor-related interneuron populations (reviewed by Bonnot et al. 2002). Converting a given neuron into a rhythmic neuron depends on the dynamic interplay between cellular and synaptic mechanisms. The most commonly used method to obtain long-lasting locomotor-like rhythms in the isolated rodent spinal cord is bath application of neurotransmitter agonists. In our study, initiating rhythmic activity was dependent on activation of NMDA, 5-HT, and dopamine receptors. The specific combination of agonists used and their concentrations determine the rhythm properties (e.g., Kiehn and Kjaerulff 1996). An example of the interactive actions of the agonists is 5-HT modulation of voltage-sensitive NMDA receptors in motoneurons of neonatal rat (MacLean and Schmidt 2001) and late embryonic and early larval *Xenopus laevis* (Sctyrngeour-Wedderburn et al. 1997). It is reasonable to assume that by activating ligand-gated channels and initiating cellular signaling cascades, the rhythmogenic cocktail recruits Hb9 INs into a pacemaker-like mode. However, the mixture of agonists probably excites numerous neuronal populations, some with functions that are not directly associated with the locomotor CPG. Therefore in the search for putative locomotor generators, it is crucial to first demonstrate the correlation between their oscillatory activity and rhythmic motor outputs. Here the hemisected spinal cord offers a significant advantage because unlike the slice preparation, motor activity can be readily monitored and correlated with rhythms induced in identified neuronal populations.

One of the criteria frequently used to classify neurons as rhythmogenic interneurons is their ability to generate membrane voltage oscillations independently of primary excitatory and inhibitory synaptic transmission. We have previously demonstrated that neurochemically induced locomotor-like rhythms in Hb9 INs persist after blocking non-NMDAR-mediated synaptic transmission (Hinckley and Ziskind-Conhaim 2006). Our new data that membrane voltage oscillations with similar frequencies were induced when primary glutamatergic transmission was blocked *before* adding the rhythmogenic cocktail indicated that fast glutamatergic connections were not required to initiate loco-

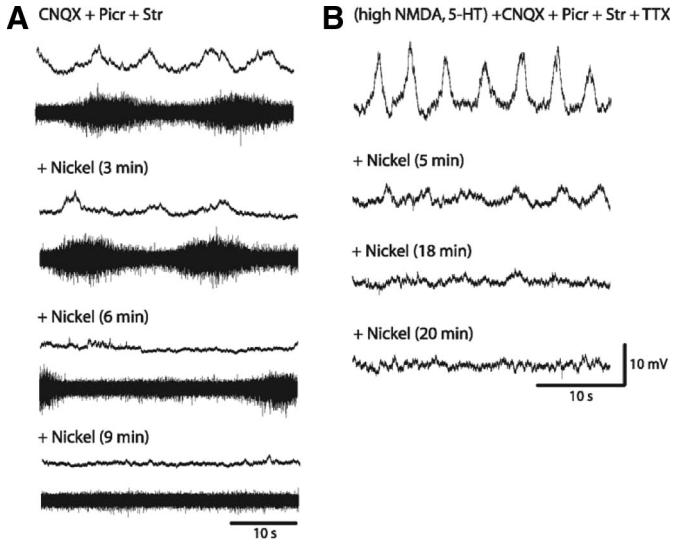

FIG. 7. Nickel suppressed neurochemically induced membrane voltage oscillations in Hb9 INs and motoneurons. *A*: in synaptically isolated Hb9 IN (CNQX + Picr + Str), bath-applied NMA (5 μM), 5-HT (10 μM), and dopamine (50 μM) induced membrane oscillations with an average amplitude of 4.6 ± 0.3 mV (SE, $n = 10$ cycles) and a frequency of 0.12 Hz. After 3-min exposure to nickel (100 μM), smaller (3.0 ± 0.3 mV) and slower (0.07 Hz) oscillations were recorded. The frequency of ventral root bursts was not altered during this time period (0.05 Hz). After 6 min, membrane oscillations were no longer detectable in Hb9 IN, but slower motor bursts persisted at lower frequency of 0.03 Hz. Rhythmic activities in the Hb9 IN and motoneurons were blocked within 9 min of nickel application. Membrane potential was –56 mV. *B*: TTX-resistant voltage oscillations were generated in synaptically isolated Hb9 IN by bath application of NMDA (20 μM), 5-HT (20 μM), and dopamine (50 μM). This is a continuation of the experiment shown in Fig. 6. The amplitude of membrane oscillation was 15.2 ± 0.4 mV at a frequency of 0.23 Hz. In the presence of nickel (5 min), the amplitude was reduced to 7.4 ± 0.04 mV (SE, $n = 20$) with a small decrease in their frequency (0.2 Hz). After 18 min, both amplitude and frequency were significantly attenuated to 3.2 mV at 0.15 Hz. Rhythmic activity was completely blocked following a 20-min exposure to nickel.

motor rhythms. Glutamatergic synaptic potentials augmented the amplitude of voltage oscillations, therefore increasing the probability of rhythmic firing. In contrast to non-NMDAR-mediated synaptic transmission, glycinergic, GABAergic, nicotinic, and muscarinic inputs did not influence the properties of membrane voltage oscillations in Hb9 INs. The observation that Hb9 IN membrane oscillations continued at the same exact frequency as locomotor rhythms following the blockade of fast synaptic transmission supports our proposal that these interneurons are functional components of the locomotor CPG.

Our study focused on the contribution of fast excitatory and inhibitory synapses to neurochemically induced locomotor-like voltage oscillations and did not address the possibility that slow synaptic transmission was involved in rhythm modulation. For example, metabotropic glutamate receptors facilitate agonists-induced rhythmic motor outputs in the neonatal rat spinal cord (Taccola et al. 2004) and modulate respiratory bursts in neurons in the pre-Bötzinger complex (Lieske and Ramirez 2006; Pace et al. 2007).

Excitatory synapses coordinate the activity between rhythmogenic interneurons and motoneurons and as demonstrated in our study, blocking the excitatory drive suppressed rhythmic motor outputs. In the presence of CNQX, inhibiting glycinergic and $GABA_A$ergic synapses triggered new episodes of slow bursting that were no longer correlated with locomotor-like voltage oscillations in Hb9 INs. This finding implied that in the absence of fast glutamatergic transmission, disinhibition unmasked alternative cellular and/or synaptic mechanisms that underlie neurochemically induced rhythmic firing in motoneurons. Exploring these mechanisms was beyond the scope of our study, but because of their long burst and interburst durations, it is unlikely that their generation was mediated by the same ligand- and/or voltage-gated inward currents that underlie membrane oscillations in Hb9 INs. It is generally assumed that the locomotor circuitry is composed of distinct neuronal populations with specific synaptic connections. However, our documentation that in the presence of rhythmogenic agonists disinhibition initiated episodes of slow motor outputs that were independent of non-NMDAR-mediated transmission might be indicative of activating redundant circuits that became predominant only after suppressing inhibitory transmission. One of the alternative explanations is that the rhythmogenic cocktail activated intrinsic signaling cascades that could be detected only after inhibitory synaptic inputs were blocked. The synchronous activity between motoneurons that was independent of primary synaptic drive can be attributed to the electrical coupling between them. It has long been recognized that prior to the formation of strong synaptic inputs in the rodent spinal cord, gap junctions between motoneurons innervating homonymous muscles synchronize their activity (Fulton et al. 1980; Walton and Navarrete 1991).

The uncorrelated rhythmic activities in Hb9 INs and motoneurons in the disinhibited hemicord differ from the report demonstrating that after blocking primary excitatory and inhibitory inputs, optically recorded rhythmic *calcium transients* in Hb9 INs were synchronous with slow bursts of motor outputs (Wilson et al. 2007). In that study, the slow rhythmic activity (cycle period: ~15 s) was induced by increasing neuronal excitability with potassium channel blockers. It is reasonable to suggest that different mechanisms underlie the small voltage oscillations in the hemisected cord that were induced by rhythmogenic agonists. To better understand the reasons for these differences, it is essential to investigate whether calcium transients were correlated with motor outputs before fast synaptic transmission was blocked.

Inward currents that participated in locomotor-like membrane oscillations in synaptically isolated Hb9 INs

Our primary finding was that locomotor-like voltage oscillations in synaptically isolated Hb9 INs were mediated via Ril- and nickel-sensitive inward currents. I_{NaP} plays an important role in the activity of neurons associated with rhythmic motor outputs controlling respiratory functions and mastication. The inspiratory neurons of the pre-Bötzinger complex are among the best-studied pacemaker interneurons in the mammalian CNS. Rhythmic activity in a fraction of this heterogeneous population is generated by I_{NaP} (Del Negro et al. 2002; Peña et al. 2004; but see Pace et al. 2007). It has been shown that the ratio between persistent sodium and potassium leak conductances determines the transition between oscillatory and quiescent states (Koizumi and Smith 2008). I_{NaP} also mediates subthreshold oscillations that underlie burst generation in the trigeminal mesencepahlic V nucleus that plays a key role in jaw movements (Enomoto et al. 2006; Wu et al. 2005).

The observation that in the presence of low NMA concentration, blocking I_{NaP} suppressed locomotor-like rhythms does not support previous reports of TTX-resistant neurochemically induced large, rhythmic membrane depolarizations in Hb9 INs in spinal cord slices of P1–P7 and juvenile mice (Han et al. 2007; Wilson et al. 2005). The rhythmic depolarizations in slices of juvenile mice were significantly faster (~1 Hz) than the 0.2-Hz locomotor-like motor outputs generated by the same neurotransmitter agonists in the *intact* spinal cord of juvenile mice (Jiang et al. 1999) and in the hemisected cord (0.1–0.2 Hz) (Hinckley and Ziskind-Conhaim 2006; Hinckley et al. 2005; reviewed by Bonnot et al. 2002). Moreover most of those fast rhythmic depolarizations were significantly larger than the 5- to 10-mV voltage oscillations recorded in the hemicord. Such large rhythmic depolarizations (>20 mV) were not detected in our previous studies, even in the presence of TEA and a higher concentration of extracellular calcium (Hinckley and Ziskind-Conhaim 2006). One of the primary differences between our study and the reports discussed in the preceding text is the concentration of NMDA in the rhythmogenic cocktail. We used only 5 μM of the racemic mixture NMA (equivalent to 2.5 μM NMDA), which is probably more physiologically relevant than the 20 μM NMDA used to induce TTX-resistant voltage oscillations. It has been shown that at high concentrations, NMDA alone can trigger TTX-resistant voltage oscillations in spinal neurons surrounding the central canal in slices of P7-14 rats (Hochman et al. 1994). The frequency of those oscillations increased as a function of NMDA concentrations. Indeed we were able to trigger large, TTX-resistant oscillations in Hb9 INs during exposure to higher NMDA concentration (20 μM) in the rhythmogenic cocktail. We demonstrated that although TTX did not block the rhythms it significantly reduced their amplitude but not their frequency (Fig. 6). It is conceivable that similar to its action on the small oscillations (Fig. 5*B*), TTX suppressed the component generated by I_{NaP}. The frequency of these large voltage oscillations was not regulated by I_{NaP}.

Slow voltage oscillations (~0.1 Hz) similar to those induced by low concentration of NMA can be triggered in the slice preparation using potassium channel blockers (Wilson et al. 2007). As shown in our study, those voltage oscillations persisted in the presence of non-NMDA, glycine, and $GABA_A$ receptors antagonists and were blocked by TTX. One of the mechanisms proposed in that study was that under these conditions intrinsic sodium conductances mediated the rhythmic activity. It should be noted that in our study fast synaptic transmission was suppressed by blocking non-NMDA, glycine, and $GABA_A$ receptors but not the release of excitatory and inhibitory neurotransmitters. Neurochemically induced regulation of endogenous glutamate, glycine, and/or GABA can affect pre- and postsynaptic cellular events associated with slow synaptic transmission. In contrast, blocking synaptic transmission by TTX suppressed action potential-dependent transmitter release. It is conceivable that different cellular mechanisms were predominant in the different experimental paradigms. For example, relatively slow (~0.2 Hz) voltage oscillations were elicited in Hb9 INs in spinal cord *slices* of P1–P7 mice (at resting membrane potential of −63 mV), and those were mostly eliminated at membrane potential of approximately −80 mV (Han et al. 2007). In the same preparation, significantly faster (~1 Hz) and larger (>20 mV) membrane oscillations were generated during simultaneous exposure to both TTX and the rhythmogenic cocktail, and their amplitude increased as a function of hyperpolarizing potentials. Therefore the neurotransmitter agonists might have triggered large calcium currents when sodium conductances were blocked.

Our observation that nickel blocked the small and large membrane oscillations in synaptically isolated Hb9 INs might suggest that LVA calcium current contributed to rhythmic activity induced by both low NMA and high NMDA concentrations. Based on the literature, the LVA calcium current is partially inactivated at resting membrane potential (e.g., Li et al. 1998), therefore it is difficult to offer a mechanistic explanation for its involvement in generating the large, nickel-sensitive voltage oscillations. Future experiments will have to examine the properties of LVA calcium currents in Hb9 INs. It has been reported that 5-HT increases LVA calcium current in rat spinal cord (Berger and Takahashi 1990), and it will be of great interest to determine whether it has a similar action on LVA calcium current in Hb9 INs. An alternative explanation for the effect of nickel on the induced oscillations is that it might suppress NMDA receptor-mediated currents as demonstrated in cultured neurons (Machete and Palazzo 2003). However, in that study, nickel blocked currents generated by high concentrations of NMDA (50 μM), and it is unknown whether it has a similar effect on the small oscillations generated by the low concentration of NMA used in our experiments.

In summary, we have previously demonstrated that Hb9 INs express several properties that are common among rhythmogenic interneurons: their neurochemically induced locomotor-like membrane oscillations are independent of fast glutamatergic transmission and electrical coupling between them (Hinckley and Ziskind-Conhaim 2006) and possibly between Hb9 INs and adjacent neurons (Wilson et al. 2007) persists during development and contributes to their synchronized activity in juvenile mice that can walk. Similar to intrinsically bursting neurons in other systems, I_{NaP} contributes to locomotor-like rhythms in synaptically isolated Hb9 INs, further supporting the intriguing concept that these locomotor-related interneurons constitute part of the rhythmogenic locomotor network in the neonatal mammalian spinal cord.

ACKNOWLEDGMENTS

We thank Dr. Meyer Jackson for valuable comments on a previous version of the manuscript.

GRANTS

This study was supported by a National Institute of Neurological Disorders and Stroke Grant NS-23808 to L. Ziskind-Conhaim.

REFERENCES

Arshavsky YU, Gelfand IM, Orlovsky GN, Pavlova GA, Popova LB. Origin of signals conveyed by the ventral spino-cerebellar tract and spino-reticulo-cerebellar pathway. *Exp Brain Res* 54: 426–431, 1984.

Atsuta Y, Garcia-Rill E, Skinner RD. Characteristics of electrically induced locomotion in rat in vitro brain stem-spinal cord preparation. *J Neurophysiol* 64: 727–735, 1990.

Berger A, Takahashi T. Serotonin enhances a low-voltage-activated calcium current in rat spinal motoneurons. *J Neurosci* 10: 1922–1928, 1990.

Bonnot A, Whelan PJ, Mentis GZ, O'Donovan MJ. Locomotor-like activity generated by the neonatal mouse spinal cord. *Brain Res Rev* 40: 141–151, 2002.

Burke RE, Degtyarenko AM, Simon ES. Patterns of locomotor drive to motoneurons and last-order interneurons: clues to the structure of the CPG. *J Neurophysiol* 86: 447–462, 2001.

Butt SJ, Kiehn O. Functional identification of interneurons responsible for left-right coordination of hindlimbs in mammals. *Neuron* 38: 953–963, 2003.

Butt SJ, Lebret JM, Kiehn O. Organization of left-right coordination in the mammalian locomotor network. *Brain Res Rev* 40: 107–117, 2002.

Butt SJ, Lundfald L, Kiehn O. EphA4 defines a class of excitatory locomotor-related interneurons. *Proc Natl Acad Sci USA* 102: 14098–14103, 2005.

Carlin KP, Dai Y, Jordan LM. Cholinergic and serotonergic excitation of ascending commissural neurons in the thoraco-lumbar spinal cord of the neonatal mouse. *J Neurophysiol* 95: 1278–1284, 2006.

Cowley KC, Schmidt BJ. A comparison of motor patterns induced by *N*-methyl-D-aspartate, acetylcholine and serotonin in the in vitro neonatal rat spinal cord. *Neurosci Lett* 171: 147–150, 1994.

Del Negro CA, Koshiya N, Butera RJ, Smith JC. Persistent sodium current, membrane properties and bursting behavior of pre-Bötzinger complex inspiratory neurons in vitro. *J Neurophysiol* 88: 2242–2250, 2002.

Enomoto A, Han JM, Hsiao CF, Wu N, Chandler SH. Participation of sodium currents in burst generation and control of membrane excitability in mesencephalic trigeminal neurons. *J Neurosci* 26: 3412–3422, 2006.

Fulton BP, Miledi R, Takahashi T. Electrical synapses between motoneurons in the spinal cord of the newborn rat. *Proc R Soc Lond B Biol Sci* 208: 115–120, 1980.

Gao BX, Stricker C, Ziskind-Conhaim L. Transition from GABAergic to glycinergic synaptic transmission in newly formed spinal networks. *J Neurophysiol* 86: 492–502, 2001.

Getting PA. Emerging principles governing the operation of neural networks. *Annu Rev Neurosci* 12: 185–204, 1989.

Goulding M, Pfaff SL. Development of circuits that generate simple rhythmic behaviors in vertebrates. *Curr Opin Neurobiol* 15: 14–20, 2005.

Han P, Nakanishi ST, Tran MA, Whelan PJ. Dopaminergic modulation of spinal neuronal excitability. *J Neurosci* 27: 13192–13204, 2007.

Hochman S, Jordan LM, MacDonald JF. *N*-methyl-D-aspartate receptor-mediated voltage oscillations in neurons surrounding the central canal in slices of rat spinal cord. *J Neurophysiol* 72: 565–577, 1994.

Hinckley CA, Hartley R, Wu L, Todd A, Ziskind-Conhaim L. Locomotor-like rhythms in a genetically distinct cluster of interneurons in the mammalian spinal cord. *J Neurophysiol* 93: 1439–1449, 2005a.

Hinckley C, Seebach B, Ziskind-Conhaim L. Distinct roles of glycinergic and GABAergic inhibition in coordinating locomotor-like rhythms in the neonatal mouse spinal cord. *Neuroscience* 131: 745–58, 2005b.

Hinckley CA, Ziskind-Conhaim L. Electrical coupling between locomotor-related excitatory interneurons in the mammalian spinal cord. *J Neurosci* 26: 8477–8483, 2006.

Hultborn H, Conway BA, Gossard JP, Brownstone R, Fedirchuk B, Schomburg ED, Enriquez-Denton M, Perreault MC. How do we ap-

proach the locomotor network in the mammalian spinal cord? *Ann NY Acad Sci* 860: 70–82, 1998.

Jiang Z, Carlin KP, Brownston RM. An in vitro functionally mature mouse spinal cord preparation for the study of spinal motor networks. *Brain Res* 816: 493–499, 1999.

Kiehn O. Locomotor circuits in the mammalian spinal cord. *Annu Rev Neurosci* 29: 279–306, 2006.

Kiehn O, Kjaerulff O. Spatiotemporal characteristics of 5-HT and dopamine-induced rhythmic hindlimb activity in the in vitro neonatal rat. *J Neurophysiol* 75: 1472–1482, 1996.

Koizumi H, Smith JC. Persistent Na^+ and K^+-dominated leak currents contribute to respiratory rhythm generation in the pre-Bötzinger complex in vitro. *J Neurosci* 28: 1773–1785, 2008.

Kuo JJ, Lee RH, Zhang L, Heckman CJ. Essential role of the persistent sodium current in spike initiation during slowly rising inputs in mouse spinal neurones. *J Physiol* 574: 819–834, 2006.

Lanuza GM, Gosgnach S, Pierani A, Jessell TM, Goulding M. Genetic identification of spinal interneurons that coordinate left-right locomotor activity necessary for walking movements. *Neuron* 42: 375–386, 2004.

Li YW, Guyenet PG, Bayliss DA. Voltage-dependent calcium currents in bulbospinal neurons of neonatal rat rostral ventrolateral medulla: modulation by alpha2-adrenergic receptors. *J Neurophysiol* 79: 583–594, 1998.

Lieske SP, Ramirez JM. Pattern-specific synaptic mechanisms in a multifunctional network. II. Intrinsic modulation by metabotropic glutamate receptors. *J Neurophysiol* 95: 1334–1344, 2006.

MacLean JN, Schmidt BJ. Voltage-sensitivity of motoneuron NMDA receptor channels is modulated by serotonin in the neonatal rat spinal cord. *J Neurophysiol* 86: 1131–1138, 2001.

Marchetti C, Gavazzo P. Subunit-dependent effects of nickel on NMDA receptor channels. *Mol Brain Res* 117: 139–144, 2003.

McCrea DA. Spinal circuitry of sensorimotor control of locomotion. *J Physiol* 533: 41–50, 2001.

Noga BR, Kriellaars DJ, Jordan LM. The effect of selective brain stem or spinal cord lesions on treadmill locomotion evoked by stimulation of the mesencephalic or pontomedullary locomotor regions. *J Neurosci* 11: 1691–1700, 1991.

Pace RW, MacKay DD, Feldman JL, Del Negro CA. Inspiratory bursts in the pre-Botzinger complex depend on a calcium-activated non-specific cation current linked to glutamate receptors in neonatal mice. *J Physiol* 582: 113–125, 2007.

Peña F, Parkis MA, Tryba AK, Ramirez JM. Differential contribution of pacemaker properties to the generation of respiratory rhythms during normoxia and hypoxia. *Neuron* 43: 105–117, 2004.

Quinlan KA, Placas PG, Buchanan JT. Cholinergic modulation of the locomotor network in the lamprey spinal cord. *J Neurophysiol* 92: 1536–1548, 2004.

Raastad M, Johnson BR, Kiehn O. Analysis of EPSCs and IPSCs carrying rhythmic, locomotor-related information in the isolated spinal cord of the neonatal rat. *J Neurophysiol* 78: 1851–1859, 1997.

Ramirez JM, Tryba AK, Peña F. Pacemaker neurons and neuronal networks: an integrative view. *Curr Opin Neurobiol* 14: 665–674, 2004.

Rekling JC, Feldman JL. Pre-Botzinger complex and pacemaker neurons: hypothesized site and kernel for respiratory rhythm generation. *Annu Rev Physiol* 60: 385–405, 1998.

Scrymgeour-Wedderburn JF, Reith CA, Sillar KT. Voltage oscillations in *Xenopus* spinal cord neurons: developmental onset and dependence on co-activation of NMDA and 5HT receptors. *Eur J Neurosci* 9: 1473–1482, 1997.

Smith JC, Ellenberger HH, Ballanyi K, Richter DW, Feldman JL. Pre-Bötzinger complex: a brain stem region that may generate respiratory rhythm in mammals. *Science* 254: 726–729, 1991.

Taccola G, Marchetti C, Nistri A. Modulation of rhythmic patterns and cumulative depolarization by group I metabotropic glutamate receptors in the neonatal rat spinal cord in vitro. *Eur J Neurosci* 19: 533–541, 2004.

Tegnér J, Hellgren-Kotaleski J, Lansner A, Grillner S. Low-voltage-activated calcium channels in the lamprey locomotor network: simulation and experiment. *J Neurophysiol* 4: 1795–1812, 1997.

Theiss RD, Kuo JJ, Heckman CJ. Persistent inward currents in rat ventral horn neurons. *J Physiol* 580: 507–522, 2007.

Tryba AK, Peña F, Ramirez JM. Stabilization of bursting in respiratory pacemaker neurons. *J Neurosci* 23: 3538–3546, 2003.

Urbani A, Belluzzi O. Riluzole inhibits the persistent sodium current in mammalian CNS neurons. *Eur J Neurosci* 12: 3567–3574, 2000.

Walton KD, Navarrete R. Postnatal changes in motoneurone electrotonic coupling studied in the in vitro rat lumbar spinal cord. *J Physiol* 433: 283–305, 1991.

Wichterle H, Lieberam I, Porter JA, Jessell TM. Directed differentiation of embryonic stem cells into motor neurons. *Cell* 110: 385–397, 2002.

Wilson JM, Cowan AI, Brownstone RM. Heterogeneous electrotonic coupling and synchronization of rhythmic bursting activity in mouse hb9 interneurons. *J Neurophysiol* 98: 2370–2381, 2007.

Wilson JM, Hartley R, Maxwell DJ, Todd AJ, Lieberam I, Kaltschmidt JA, Yoshida Y, Jessell TM, Brownstone RM. Conditional rhythmicity of ventral spinal interneurons defined by expression of the Hb9 homeodomain protein. *J Neurosci* 25: 5710–5719, 2005.

Wu L, Ziskind-Conhaim L. Commissural GAD67 interneurons are constituents of rhythm-coordinating networks in the mouse spinal cord. *Soc Neurosci Abstr* 252.12, 2006.

Wu N, Enomoto A, Tanaka S, Hsiao CF, Nykamp DQ, Izhikevich E, Chandler SH. Persistent sodium currents in mesencephalic v neurons participate in burst generation and control of membrane excitability. *J Neurophysiol* 93: 2710–2722, 2005.

Zar JH. Circular distribution. In: *Biostatistical Analysis,* edited by McElroy WD, Swanson CP. Englewood Cliffs, NJ: Prentice-Hall, 1974, p. 310–327.

Zhong G, Diaz-Rios M, Harris-Warrick RM. Intrinsic and functional differences among commissural interneurons during fictive locomotion and serotonergic modulation in the neonatal mouse. *J Neurosci* 26: 6509–6517, 2006.

Zhong G, Masino MA, Harris-Warrick RM. Persistent sodium currents participate in fictive locomotion generation in neonatal mouse spinal cord. *J Neurosci* 27: 4507–4518, 2007.

Ziskind-Conhaim L, Gao BX, Hinckley C. Ethanol dual modulatory actions on spontaneous postsynaptic currents in spinal motoneurons. *J Neurophysiol* 89: 806–813, 2003.